# Rates of Flow Through Microporous Solids

**E. R. GILLILAND, R. F. BADDOUR, and J. L. RUSSELL**

**Massachusetts Institute of Technology, Cambridge, Massachusetts**

**Rates of flow of pure gases, both those with no adsorption and those with appreciable adsorption, were studied as a function of pressure level, pressure drop, and temperature for flow through 1/2-in.-diameter cylindrical plugs of activated carbon and of unsintered Vycor glass. Adsorption isotherms for the pure gases on Vycor glass were measured over the range of variables covered in the flow studies. A few measurements were made for bulk liquid flowing through a Vycor plug.**

**Permeabilities, which are proportional to the rate of flow per unit of pressure drop, were satisfactorily correlated for hydrogen, helium, argon, and nitrogen by employing existing gas-phase flow theory. Permeabilities considerably larger than the values predicted from the nonadsorbed gas correlation, sometimes more than seventeen times as large, were observed for ethylene, propylene, and isobutane flowing through a Vycor plug. For the hydrocarbon-Vycor systems, permeabilities for vapor flow are as much as sixty times larger than for bulk liquid flow.**

**The unusual flow phenomena for the hydrocarbon-Vycor systems are attributed to a rapid transport in the adsorbed layer. The total transport is treated as being the sum of gas-phase and adsorbed-layer flow. An equation describing adsorbed-layer movement is derived by utilizing a force balance together with thermodynamic principles. The resulting equation has just one empirical constant, and its use requires adsorption-isotherm data. It correlates very well the surface flow rates for the major range of the variables covered in this investigation. Rate measurements were made for adsorbed-layer concentrations ranging from about one tenth of a monolayer up through the capillary condensation region. Deviations in the one constant form of the equation are observed below one tenth of a monolayer. The available literature data on flow in adsorbed layers are reasonably well correlated by the same equation.**

A number of processes used in industry today involve the transport of gas within the structure of microporous solids. Catalytic reactors, adsorption units, and gaseous separation barriers are typical units in which these solids are utilized. Satisfactory techniques exist in the literature for predicting nonadsorbed-gas flow rates through these solids; however, for many processes the gas adsorbs on the solid and it is possible for a net migration to occur both in the gas phase and in the adsorbed layer. Very few definitive data are available on rates of movement within the adsorbed layer, and even less is known about the mechanism of this movement.

It was the major purpose of this investigation to study the main variables affecting transport in adsorbed layers and to develop a better quantitative and qualitative understanding of the nature of this flow. Sounder fundamental knowledge of the phenomenon should result in better correlations of rates of adsorbed-gas flow and subsequently in better design procedures for commercial units.

## DEVELOPMENT OF SURFACE-FLOW EQUATION

A mathematical picture is developed below for transport in adsorbed layers by use of fundamental dynamic and thermodynamic principles. The derivation presented below employs a two-dimensional force balance on an adsorbed film; an alternative approach employs a mechanical-energy balance on the adsorbed layers (*20*).

Fowler and Guggenheim (*13*) and others, in statistical treatments of adsorption, have assumed that adsorbed films have a two-dimensional property analogous to the pressure of a three-dimensional gas phase. This property $\phi$ is called the *spreading pressure*. It represents the force per unit width necessary to compress the adsorbed film, or conversely that needed to keep it from spreading over clean surface.

Using the concept of a spreading pressure and assuming that the shear stress between the adsorbed layer and the solid is proportional to the average rate of movement of adsorbed molecules past the surface, one may make a force balance on the film

$$-uC_R\,dl = d\phi \qquad (1)$$

This balance neglects any shear stress between the adsorbed layer and the gas phase.

Babbitt (*1*) proposed a relation of the

---

J. L. Russell is at present with Dow Chemical Company, Midland, Michigan.

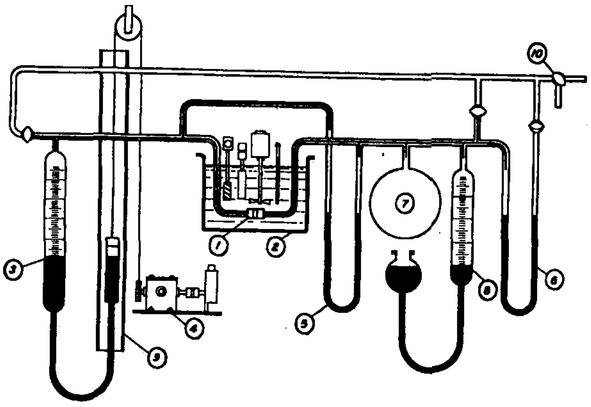

Fig. 1. Pure-gas-flow-rate apparatus.

same form as Equation (1) for describing flow of gases through so-called "nonporous" solids, e.g., metals. Using a relation between $\phi$ and the amount adsorbed that was derived statistically, he analyzed a limited number of data for hydrogen flow through iron and copper as a function of pressure level. His relation satisfactorily explained the shape of the curves of flow rate vs. pressure level.

In order to develop a general relation between $\phi$ and the concentration in the adsorbed layer, a solid-gas system at isothermal equilibrium is considered. For such a system it can readily be shown that

$$d\bar{F}_G = d\bar{F}_s \qquad (2)$$

It can be deduced from the properties of $\phi$ that

$$\frac{(\partial \bar{F}_s)}{(\partial \phi)}_T = A_m \qquad (3)$$

With the assumption that the perfect gas law is applicable, Equations (2) and (3) may be transformed to

$$RT\frac{dp}{p} = A_m\, d\phi = \frac{1{,}000 s_s\, d\phi}{x} \qquad (4)$$

If it is assumed that equilibrium exists between the gas phase and the adsorbed layer during flow, Equations (1) and (4) may be combined to give the desired form of a general equation for flow of an adsorbed layer.

$$u = -\frac{RT}{1{,}000 C_R s_s}\,\frac{x}{p}\,\frac{dp}{dl} \qquad (5)$$

It is noted that Equation (5) contains a free-energy gradient as the potential for flow. Either $\bar{F}_G$, $\bar{F}_s$, or $\bar{F}_{ads}$ may be used as the gradient, where $\bar{F}_{ads}$ is the total free energy of the adsorbed nolecules per mole of adsorbate.

In applying Equation (5) to flow through a microporous solid plug, one assumes that the adsorbed layer travels in a tortuous path along the actual pore lengths. This effect can be accounted for by

$$dl = k\, dl_p \qquad (6)$$

Also

$$u_p = \frac{u}{k} \qquad (7)$$

The adsorbed-layer transport through a cylindrical plug, for flow normal to its faces, is related to the average net velocity of the adsorbed film $u_p$ by

$$\frac{N_s}{A_p} = x\rho_{app}u_p \qquad (8)$$

Combining Equations (5) through (8) and integrating for the case where both $N_s$ and the product $C_R s_s$ are constant results in the following relation:

$$\frac{N_s}{A_p} = \frac{RT\rho_{app}}{1{,}000k^2 C_R s_s L_p}\int_{p_2}^{p_1}\frac{x^2}{p}\,dp \qquad (9)$$

In the derivation of Equation (9) it is also assumed that resistances to flow at the two interfaces, such as adsorption-desorption resistances, are negligible compared with the resistance inside the plug.

For special isotherm cases it is possible to integrate Equation (9) directly. Several such integrations have been made (*20*). The utility of Equation (9) can best be evaluated in the light of experimental results on adsorbed-layer flow.

## EXPERIMENTAL

Experimentally, rates of flow of pure gases, both nonadsorbed and appreciably adsorbed, were studied as a function of pressure level, pressure drop, and temperature for flow through ½-in.–diameter cylindrical plugs of activated carbon and of unsintered Vycor glass. A sketch of the apparatus employed in these measurements is shown in Figure 1.

In essence, the experimental technique consisted of flowing a pure gas through a porous plug that was held in neoprene tubing (1) immersed in a constant-temperature bath (2). After a pure gas was introduced through the stopcock (10), constant-volume sections on both sides of the plug were closed, and mercury was fed into an upstream burette (3), thus forcing gas through the plug. Owing to a large volume downstream (7), the downstream pressure (6) was relatively insensitive to the flow and was maintained constant during a run by leveling bulb (8). Runs were continued until the pressure drop (5) attained the steady state value corresponding to the permeability of the plug for the operating conditions. At steady state the volumetric rate of gas flow through the plug, at the upstream pressure and temperature, equaled the constant rate of mercury flow into the upstream burette, as controlled by a constant-speed motor (4), which lifted a cylinder of mercury at a constant rate up a guide rack (9). The very low volumetric flow rates, 0.4 to 350 cc./hr., necessitated the use of a volumetric displacement technique for measuring rates.

Tests with steel plugs illustrated that any combined flow through the tubing, and between the steel plugs and the tubing, was negligible relative to rates through the porous plugs. Flow between the porous plugs and the tubing was also shown to be insignificant by evaluation of the non-adsorbed-gas flow mechanisms and by illustrating reproducibility in different tubing environments.

Flow rates of hydrogen, helium, argon, and nitrogen through the two types of plugs were studied over a mean pressure-level range of a few mm. Hg to about 1,130 mm. Hg, a pressure-drop range of a few mm. Hg to about 385 mm. Hg, and a temperature range of 25° to 85°C. These gases were considered to be negligibly adsorbed. Measurements for isobutane flowing through a carbon plug at 25°C, were made over an approximate mean pressure range of 8 to 630 mm. Hg. Rate studies were made with ethylene, propylene, and isobutane flowing through a Vycor plug at 0°, 25°, and 40°C. For these measurements the mean pressure varied from about 10 to 1,100 mm. Hg and pressure drops varied from about 3 to 725 mm. Hg. A measurement of the bulk liquid rate for isobutane flow through the Vycor plug was made at 0°C. Also, the bulk liquid rate of isooctane flow through the Vycor plug was determined by forcing the liquid through the plug at room temperature and under nitrogen pressure.

Adsorption isotherms for the pure hydrocarbon gases on Vycor glass were measured over the range of variables covered in the adsorbed-gas rate studies. Effects of particle size on the isotherms were studied over a range of 10 to 200 mesh. In addition, the plug used for the rate studies was later ground up for a further check on the isotherms. The equipment employed for the equilibrium studies was a standard constant-volume apparatus. Nitrogen-surface areas and porosities of the two solids were independently determined by standard techniques. All the original data are on file (*20*).

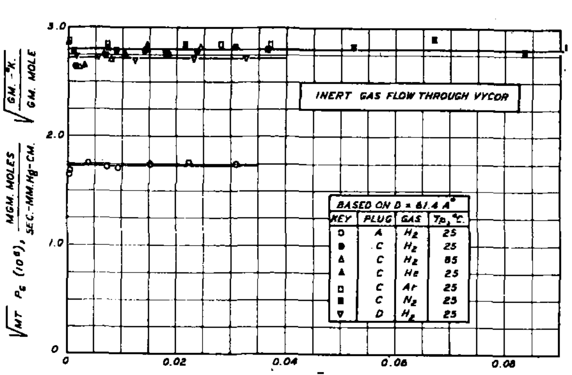

Fig. 2. Inert-gas flow through Vycor.

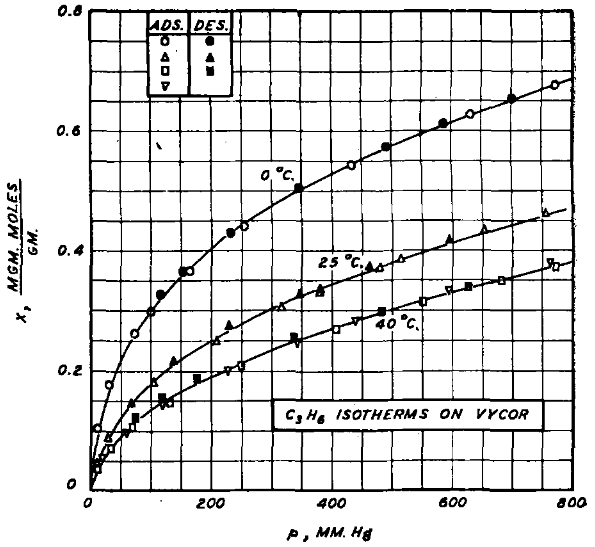

Fig. 3. $C_3H_6$ isotherms on Vycor.

## RESULTS AND DISCUSSION

### 1. Nonadsorbed Gas Rates

*Carbon.* The mechanism of nonadsorbed-gas flow through activated-carbon plugs has the characteristics of slip flow. The results are satisfactorily correlated (*20*) by a form of the slip-flow equation suggested by Carman and Arnell (*4*). A slight increase in rates above the slip-flow correlation was observed at low pressures and is similar to that observed by Carman (*4*) for nonadsorbed-gas flow through compressed-powder beds.

*Vycor.* Measurements for the flow of nonadsorbed gases through several Vycor plugs are presented in Figure 2. The Vycor plug discussed hereafter, plug C, had a cross-sectional area of 1.412 sq. cm. and a thickness of 0.372 cm. The data are plotted and correlated in a manner suggested by the molecular-flow equation, derived by Knudsen (*19*) for a gas flowing down a capillary of radius $r$ and length $L$, as

$$\frac{N_G}{1{,}000}=\frac{8}{3}\,\frac{\pi r^3}{\sqrt{2\pi RTM}}\,\frac{(2-f)}{(f)}\,\frac{\Delta p'}{L} \tag{10}$$

The main criterion for molecular flow is that the capillary diameter be small compared with the mean free path of the gas at the mean pressure level. In the abscissa in Figure 2 $D$ is the average pore diameter of the porous glass, which is believed to be reasonably uniform. The value of $D$ = 61.4 Å. for Vycor was determined from nitrogen adsorption and mercury-helium density measurements. The mean free path was calculated from Equation (11), which is a transformation of a relationship given by Jeans (*18*):

$$\bar{\lambda} = \frac{3\mu}{\bar{p}'\sqrt{M}}\sqrt{\frac{\pi RT}{8}} \tag{11}$$

The maximum deviation of the data from the constant value for $\sqrt{MTP_G}$ is about ±5% and the mean deviation is approximately ±2%. $P_G$ is the gas phase permeability $(N_G L_p)/\Delta P A_p$. Since the ordinate does not depend on $\lambda$, the gas-phase flow rates do not depend on pressure level or the gas viscosity. In addition the mole flow rates per unit pressure drop vary inversely as $\sqrt{MT}$. These characteristics lead to the conclusion that molecular flow is the main mechanism of gas-phase transport through Vycor for the range of variables covered.

The correlation in Figure 2 and Equation (10) has been combined with a pore model for Vycor similar to that employed by Barrer (*2*), to evaluate pore-structure characteristics. This model is comprised of parallel capillaries of equal radii which travel in tortuous paths and have a tortuosity factor $k$ equal to 2.56 (*3*). With a value for the porosity of 0.31 and for the real solid density of 2.05, the internal surface area of the Vycor plug C may be calculated to be 118 ($10^4$) sq. cm./g. This compares favorably with a value of 143 ($10^4$) sq. cm./g. as determined by nitrogen adsorption.

### 2. Equilibria

Some adsorption isotherms for the hydrocarbons on Vycor are given in Figures 3 and 4. Adsorption points are those taken with an increasing pressure level between runs and desorption points are those taken with a decreasing pressure level. The mean deviation of the points from the curves is ±2%. Isotherm values are not affected appreciably by particle size. Data on the plug employed in the rate studies are within a few per cent of those shown in Figures 3 and 4.

For the isobutane isotherm at 0°C., shown in Figure 4, a hysteresis loop is observed which is similar to other capillary condensate regions reported for Vycor (*10*). The closing of the hysteresis loops and the flattening of the isotherm above about 950 mm. Hg indicates a saturation condition within the pores. At an amount adsorbed of 2.03 mg. moles/g., with the density of the adsorbed phase being assumed equal to the bulk-liquid density, the volume of adsorbed phase per unit of total volume is equal to 0.286. Since this is close to the porosity value of 0.31, it is concluded that the voids are full of isobutane in a state similar to its bulk-liquid form.

Heats of adsorption increase in the order of ethylene, isobutane, and propylene. This illustrates that the unsaturation or polarity effect plays a major part in adsorption on Vycor.

### 3. Absorbed Gas Rates

*Carbon.* Permeability measurements, taken for isobutane flowing through the carbon plug, are satisfactorily predicted by the nonadsorbed-gas correlation because of a large gas-phase flow through macropores, which masks any surface-flow contribution to the total rates. If the gas-phase component were reduced, as in a bulk diffusion system, it might be possible for the surface flow to be appreciable.

The plugs were made of bonded carbon particles and the extra voids encountered between particles would markedly increase the gas-phase rate. Flood and Tomlinson (*11*, *12*, *22*) have observed appreciable surface rates for pure adsorbed-gas flow through solid-carbon rods.

*Vycor.* Data for the total flow rates of hydrocarbons through Vycor are presented in Figures 5 and 6 for $C_3H_6$ at 0°, 25°, and 40°C., and for $i$-$C_4H_{10}$ at 0°C. Some sample data are presented in Table 1. The remaining data are on file (*20*). The predicted ordinate, based on the nonadsorbed-gas correlation, is shown and the dashed lines represent extrapolations of the correlation. It is obvious that the data are not adequately predicted by this correlation.

Hydrocarbon permeabilities are considerably larger than the values predicted from a nonadsorbed-gas correlation, sometimes being more than seventeen times as large. The permeabilities vary considerably with pressure level and increase rapidly as the temperature is lowered. In addition, the effects of pressure at low mean pressures are unusual. For the hydrocarbon-Vycor systems, permeabilities at pressures below the vapor pressure are greater than bulk-liquid permeabilities, sometimes being more than forty to sixty times as large. It is clear that the flow does not have the characteristics of normal diffusion.

In Figure 6 the solid curves are the best ones through the adsorption and desorption points, respectively. The observed hysteresis occurs over a pressure range comparable to the one found in the equilibrium curve, shown in Figure 4. The permeability of isobutane at 0°C., just below the vapor pressure, where the voids of Vycor are approximately full of a liquidlike phase, is about forty times that observed for bulk-liquid flow just above the vapor pressure. If a pore model is employed for Vycor, the bulk-liquid permeabilities of isobutane and isooctane may be predicted by Poisseuille's Law (*20*).

In an analysis of the possible causes of the deviations observed with the hydrocarbon-Vycor systems (*20*), the flow phenomena are attributed to a rapid transport in the adsorbed layer itself. The ratios of surface to gas-phase flow are high enough to allow a reliable quantitative analysis to be made for surface flow with the following assumptions. Any net flux between the gas phase and the adsorbed layer is neglected and surface rates are evaluated as the difference between the total rates and the values predicted by the nonadsorbed-gas correlation; a correction factor is applied to the gas-phase prediction which estimates the effect of the adsorbed layer in blocking off cross-sectional area available for gas-phase flow. The simplest case for this blocking is assumed, namely, that the adsorbed layer is distributed uniformly over the surface of the Vycor and that the density of the adsorbed phase equals the bulk-liquid density.

## GENERAL DATA TREATMENT

Equation (9) predicts that a plot of $N_s L_p/A_p$ vs $\int_{p_2}^{p_1} (x^2/p)\, dp$ should give a straight line through the origin. Typical plots of this nature are given in Figures 7 and 8. These figures were constructed by utilizing the surface-flow rates calculated from Figures 5 and 6 and the isotherm curves given in Figures 3 and 4. In general, the order of points along the abscissas are the same as in Figures 5 and 6.

The solid lines in Figure 7 are the best straight lines through the origin fitting the results above $\bar{x} = 0.06$, corresponding to about one-tenth of a monolayer. A point was obtained at $N_s L_p/A_p = 7.07\ (10^{-6})$ and $\int_{p_2}^{p_1} (x^2/p)\, dp = 15.02\ (10^{-2})$ which is about 8% below an extension of the line for 0°C. points. Above the $\bar{x} = 0.06$ the maximum deviations from such straight lines for ethylene and propylene are about ±30% for two points. For approximately fifty other points the maximum deviation runs about ±10 to 15%, and the mean deviation is approximately ±6 to 7%. For the limited amount of data below $\bar{x} = 0.06$ for ethylene and propylene, ranging down to about one-fortieth of a monolayer, the points are consistently above the correlating line drawn for higher amounts adsorbed. The points below $\bar{x} = 0.06$ correspond to the lowest pressure runs in Figure 5. Such data points are as much as 2.5 times the straight-line value.

For the isobutane results plotted in Figure 8, the solid line is the best line through the origin fitting the points above $\bar{x} = 0.09$, corresponding to above about one-fifth of a monolayer. The mean deviation from such lines above $\bar{x} = 0.09$ for all the isobutane measurements, including about thirty points, is about ±12%. As observed with ethylene and propylene, the points at very low amounts adsorbed are considerably higher than the straight lines used in correlating the data at higher amounts adsorbed. Below $\bar{x} = 0.09$, down to one-thirtieth to one-fortieth of a monolayer, points at 25° and 40°C. for isobutane are as much as five to six times the values given by the straight lines drawn.

Of particular interest is the fact that the one constant form of the hydrodynamic equation, Equation (9), satisfactorily correlates the results presented in Figure 8 from less than about one-fifth of a monolayer up through the hysteresis region to a condition where the voids are full of a liquidlike phase.

The derivation of Equation (9) did not employ any assumptions as to the degree to which the capillaries were filled with adsorbed phase. It was assumed that if a gas phase is present, any shear due to gas flow is negligible. The velocity of adsorbed-phase transport in Equation (5) is simply taken to be proportional to the spreading pressure gradient or to a free-energy gradient. Apparently, the proportionality constant, which is thought to be a measure of the resistance to flow at the solid-boundary layer, is the same with the isobutane-Vycor syxtem for all levels of adsorption above one-fifth of a monolayer, including the condition of full capillaries.

At first sight, the high permeabilities just below the vapor pressure seem anomolous relative to the low bulk-liquid permeabilities just above the vapor pressure. It is possible to understand this phenomenon by considering the work input in the two cases. The molal-free-energy change per unit pressure drop is much larger in taking a mole from one face of the plug to the other when vapor is present at the faces than when bulk liquid is present. In other words, the spreading pressure gradient across the plug is considerably greater in the former case. This leads to the conclusion that the high rates just below the vapor pressure are obtained at the expense of a greater work input. Thus, as might be expected, it is possible that the energy dissipation per unit of flow through the plug is approximately the same just above and below the vapor pressure.

It is concluded that Equation (9) correlates very well the surface-flow rates for the major range of variables covered in this investigation.

## LOW $\bar{x}$ DEVIATION

The deviations from the correlation at very low amounts adsorbed imply that the resistance to movement in very dilute surface concentrations is less than that at higher amounts adsorbed. A possible surface-flow mechanism which is consistent with the observed low resistance to flow is that the force fields of neighboring high-energy sites overlap, and at low amounts adsorbed, where the neighboring high-energy sites are empty, migration occurs along a low-resistance path from high-energy site to high-energy site. When the high-energy sites begin to fill as adsorption is increased, the movement will tend to be from high to low in view of the fact that neighboring high-energy sites are occupied and not immediately available to a molecule. The experimental results indicate that the resistance of the path from high to high is less than the average resistance afforded by the actual paths to and from both high- and low-energy sites when higher amounts are adsorbed. Further experimental work is necessary to correlate adequately the transport at very low amounts adsorbed.

## EFFECT OF $\Delta p$

In general, Equation (9) predicts that the surface-flow rate per unit of gas-phase pressure drop will depend upon the pressure drop. The observed surface permeabilities for hydrocarbons did not show a detectible change with pressure gradient over the range employed, which was relatively small. For the conditions of these tests and the isotherms involved, $\int_{p_2}^{p_1} (x^2/p)\, dp \cong (\bar{x}^2/\bar{p})\, \Delta p$, which masks any pressure-drop effect. Consequently, the data do not provide an adequate test of the effect of pressure drop.

## EFFECT OF TEMPERATURE AND GAS PROPERTIES

On the assumption that $s_s$ is constant and equal to the specific surface, as measured by nitrogen adsorption, $C_R$'s

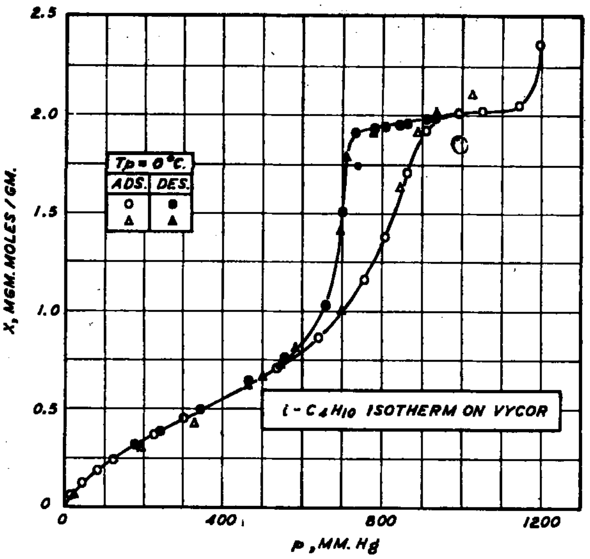

Fig. 4. $i - C_4H_{10}$ isotherm on Vycor.

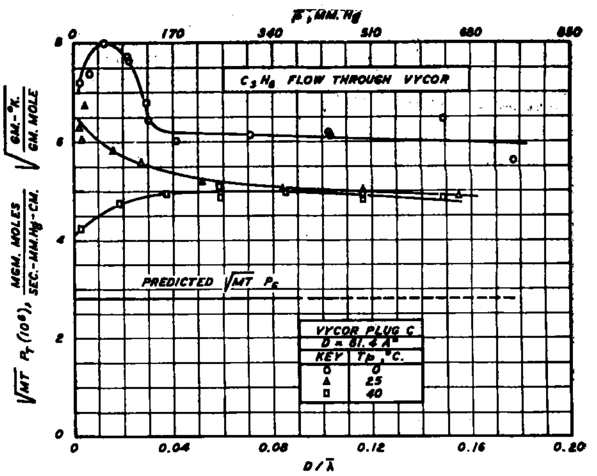

Fig. 5. $C_3H_6$ flow through Vycor.

may be evaluated from the slopes of the lines in plots like Figures 7 and 8 with Equation (9). The coefficient of resistance is believed to be characteristic of only the nature of the solid surface and the adsorbed molecule. The coefficients of resistance decrease rapidly as temperature increases, and the effect is well correlated by an Arrhenius type of equation. Figure 9 shows a plot of ln $C_R$ vs. $1/T$ for ethylene, propylene, and isobutane on Vycor. For all the hydrocarbons, activation energies are approximately 3,000 cal./g. mole, and the ratio of the activation energy to the heat of adsorption varies from about 0.4 to 0.5.

The resistance coefficient at $1/T = 0$, $C_{R_0}$, increases in the order of ethylene, isobutane, and propylene. Heats of adsorption increase in the same order, showing that the magnitude of the attractive forces between the solid and the absorbed layer plays a major role in determining flow rates in adsorbed layers.

## LITERATURE DATA

Numerous investigators have observed phenomena attributed to movement of an adsorbed layer through microporous solids (*3, 5, 6, 7, 11, 12, 14, 15, 16, 17, 22, 23, 24, 25*). Perhaps the most reliable quantitative values for surface flow that are available are the results of Carman and coworkers (*5, 6, 7*) and some of the measurements of Flood and Tomlinson (*11, 12*). These data have been analyzed (*20*) and the surface-flow rates are reasonably well correlated by Equation (9) for a fairly wide range of conditions. Presented in Table 2 are coefficient-of-resistance values for some of these literature data that are well correlated by Equation (9). Values extrapolated from Figure 9 are also given for comparison with the present results at comparable temperatures.

In view of Carman's data for pure adsorbed gas flow through compressed-powder beds, $C_R$'s for surface flow of difluorodichloromethane through a silica-powder bed fall between values for isobutane and propylene on a Vycor (silica) plug at comparable temperatures. Reported values (*7*) for the heats of adsorption of difluorodichloromethane on the silica powder also fall between those obtained for isobutane and propylene on Vycor, for comparable fractions of surface covered. A coefficient of resistance for difluorodichloromethane flowing through a compressed–carbon-black–powder bed is larger than the $C_R$'s obtained in this investigation at a comparable temperature, as is the measured heat of adsorption. As in the present studies, data below about one-fifth of a monolayer on the compressed beds, including surface-transport measurements for carbon dioxide, are consistently higher than predicted by Equation (9). The ratio of surface rates to the value predicted by Equation (9) increases as the amount adsorbed decreases. Surface rates in a capillary condensate region for difluorodichloromethane and sulfur dioxide moving through a silica-powder bed are not satisfactorily correlated by the one constant form of the hydrodynamic equation at higher amounts adsorbed. As the amounts adsorbed increase in the capillary condensate region, the surface rates become increasingly larger than the values extrapolated from data at lower

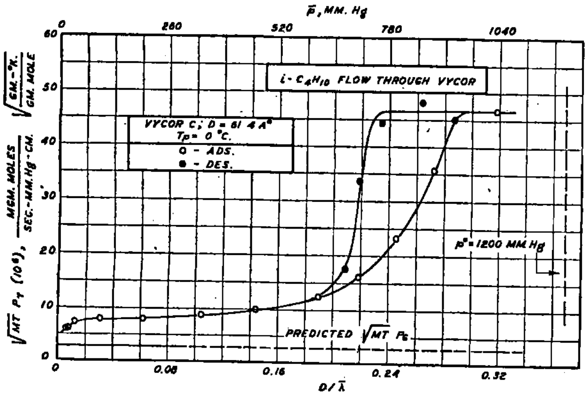

Fig. 6. $i - C_4H_{10}$ flow through Vycor.

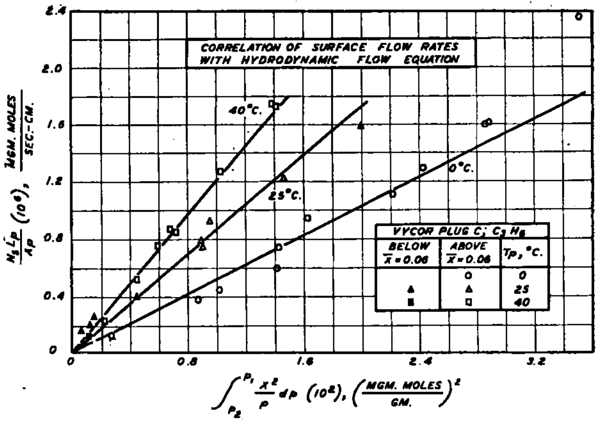

Fig. 7. Correlation of surface flow rates with hydrodynamic flow equation.

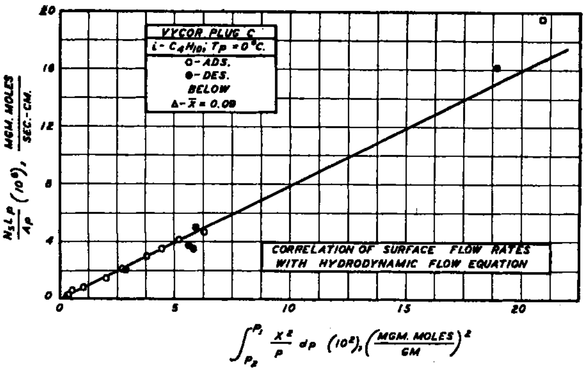

Fig. 8. Correlation of surface flow rates with hydrodynamic flow equation.

amounts adsorbed by means of Equation (9). In general, it might be expected that the resistance to surface transport would tend to decrease as the thickness of the adsorbed layer increased, or as a greater portion of the molecules were moving outside the influence of the surface-force fields.

Adsorbed-layer rates in a capillary condensate region for flow of water through an activated-carbon rod (*11*, *12*) are satisfactorily correlated by Equation (9).

It is concluded that Equation (9) correlates literature data for a range of conditions wide enough to illustrate its utility very well. More data are needed to define the variation in the resistance coefficient at very low amounts adsorbed and for some of the capillary-flow data. The reasonable and consistent variation in the $C_R$'s given in Table 2 indicates that Equation (9) correctly characterizes the physical factors involved for conditions where it is applicable.

TABLE 1

SAMPLE DATA, $i$ – $C_4H_{10}$ AT 0°C.

Adsorption Points

| $\bar{p}$, mm.Hg | $\Delta p$, mm.Hg | $\bar{x}$, mg. moles/g. | $\frac{N_T}{\Delta p}$ $(10^7)$, mg. moles/(sec.)(mm.Hg) |
|---|---|---|---|
| 20.5 | 10.2 | 0.072 | 1.74 |
| 22.6 | 10.8 | 0.077 | 1.81 |
| 41.2 | 16.7 | 0.116 | 2.09 |
| 103 | 9.3 | 0.216 | 2.29 |
| 203 | 17.9 | 0.35 | 2.36 |
| 342 | 27.1 | 0.51 | 2.61 |
| 469 | 32.6 | 0.63 | 2.96 |
| 618 | 34.1 | 0.83 | 3.71 |
| 712 | 30.0 | 1.03 | 4.82 |
| 799 | 23.1 | 1.34 | 6.98 |
| 887 | 16.5 | 1.84 | 10.8 |
| 1,033 | 52.8 | 2.03 | 14.1 |
| Desorption Points | | | |
| 937 | 14.0 | 1.99 | 13.6 |
| 859 | 42.2 | 1.97 | 14.6 |
| 766 | 11.6 | 1.93 | 13.4 |
| 712 | 14.2 | 1.69 | 10.2 |
| 679 | 26.0 | 1.24 | 5.32 |

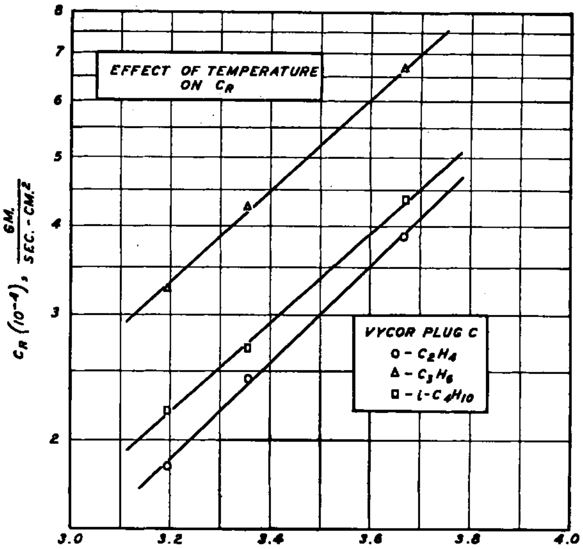

Fig. 9. Effect of temperature on $C_R$.

## FICK'S LAW

Another possible method of correlating the absorbed-layer flow values is with Fick's Law, which has been almost invariably taken to apply by previous workers (*3*, *6*, *7*, *8*, *9*, *14*, *21*, *23*). Recently (*12*, *23*) the case for flow in a capillary which is full of condensed phase has been treated as a modified type of Poiseuille's Law transport.

For surface transport through a porous plug with tortuous transport paths, an integrated form of Fick's Law is

$$\frac{N_s}{A_p} = D_s \frac{\rho_{app}}{k^2} \frac{\Delta x}{L_p} \qquad (12)$$

Typical surface diffusivities are given in Figures 10 and 11 for the propylene runs and for isobutane at 0°C. All points are shown except those corresponding to the four highest rate measurements given in Figure 6 for isobutane, when the plug voids were approximately full of adsorbed phase. It was inconvenient to place these points on the figure as they are far off scale. If Equation (12) is applied to these four points, diffusion coefficients of approximately 5 $(10^{-3})$ sq. cm./sec. at $\bar{x}$ = 2 are obtained. The solid lines represent the best curves through the plotted points.

The surface diffusivities for all the hydrocarbons vary greatly with the amount adsorbed. Generally the diffusivities rise rapidly when the amount adsorbed corresponds to less than a monolayer, as in Figure 10 and up to about $\bar{x}$ = 0.45 in Figure 11. For these regions the diffusivities often increase as much as tenfold over the range of concentrations covered. Above a monolayer, as seen in Figure 11, the diffusivity goes through a maximum and minimum and is appreciably different for adsorption and desorption runs at a given $\bar{x}$. When diffusion coefficients vary in such a manner with concentration, the utility of the concept of a diffusivity, as it is normally defined, has been lost for correlating purposes. Surface diffusivities calculated from the correlation with Equation (9) are represented by the dashed curves in Figure 11.

It is concluded that Equation (9), which is based on a force-balance derivation, is a more satisfactory means of correlating surface-rate data than are previous approaches which employ diffusion coefficients.

## CONCLUSIONS AND RECOMMENDATIONS

1. Permeabilities of pure adsorbed gases through microporous solids are often considerably higher than values predicted from correlations based on non-adsorbed-gas-flow data. The deviations are due to a transport in the adsorbed

TABLE 2

COEFFICIENTS OF RESISTANCE

| Investigator | System | $T_p$, °C. | $C_R(10^{-5})$, g./(sec.)(cm.$^2$) |
|---|---|---|---|
| (*7*) | $CF_2Cl_2$-carbon-black–powder bed | −21.5 | 1.32 |
| | | 20 | 1.02 |
| (*7*) | $CF_2Cl_2$-silica-powder bed | −33.1 | 1.22 |
| | | −21.5 | 0.85 |
| (*11*),(*12*) | $H_2O$-activated-carbon rod | 35 | 11.8 |
| (*20*) | *Vycor (silica) ethylene | −33.1 | 0.88 |
| | | −21.5 | 0.65 |
| (*20*) | *Vycor (silica) propylene | −33.1 | 1.43 |
| | | −21.5 | 1.07 |
| (*20*) | *Vycor (silica) isobutane | −33.1 | 0.91 |
| | | −21.5 | 0.69 |

---

*Extrapolated values.

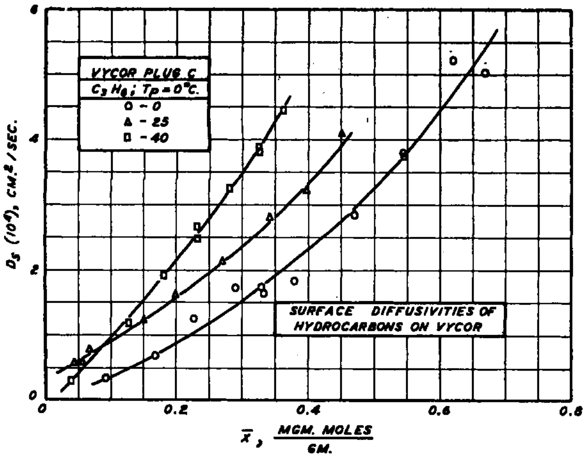

Fig. 10. Surface diffusivities of hydrocarbons on Vycor.

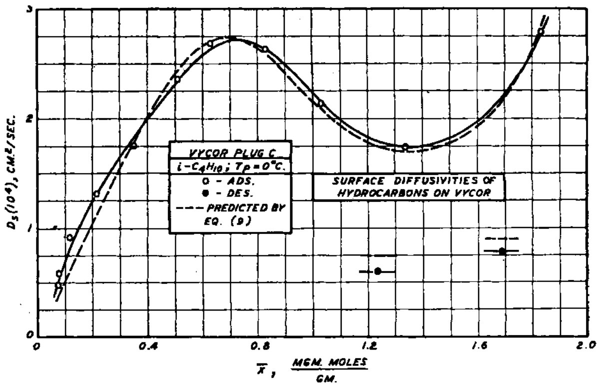

Fig. 11. Surface diffusivities of hydrocarbons on Vycor.

layer, which can often be a major portion of the total transport and can even be the controlling mechanism of flow.

2. An equation for surface flow has been developed which is related to general isotherm values and one empirical constant, by considering the movement in the adsorbed layer to be a hydrodynamic phenomenon. This equation satisfactorily correlates available surface-flow data for a wide range of conditions, and upon being combined with existing gas-phase–transport theories, total adsorbed-gas rates are satisfactorily correlated.

3. Further experimental data are required to study quantitatively deviations from the one constant form of the hydrodynamic equation. It is recommended that the force-balance approach to adsorbed-phase flow be applied to the flow of gases through so-called "nonporous" solids, such as plastic membranes and metals.

## ACKNOWLEDGMENT

This work was accomplished with the aid of fellowships from the E. I. duPont de Nemours and the Eastman Kodak companies.

## NOTATION

$A_m$ = total area over which adsorbed molecules are mobile, per mole of adsorbate, sq. cm./g. mole

$A_p$ = plug cross-sectional area, sq. cm.

$C_R$ = coefficient of resistance, g./(sec.)(sq. cm.)

$C_{R_0}$ = coefficient of resistance at $1/T = 0$, g./(sec.)(sq. cm.)

$D$ = diameter of capillary or pore, cm.

$D_S$ = surface diffusivity, sq. cm./sec.

$f$ = fraction of molecules emitted diffusely after collision

$\bar{F}_{ads}$ = free energy of the molecules in the adsorbed layer, per mole of absorbate, ergs/g. mole

$\bar{F}_G$ = molal free energy in gas phase, ergs/g. mole

$\bar{F}_S$ = total free energy of the solid and the adsorbed molecules, per mole of adsorbate, ergs/g. mole

$k$ = tortuosity factor

$l$ = distance along surface in direction of flow, cm.

$l_p$ = distance in direction of net flux, or along axial length of plug, cm.

$L$ = capillary length, cm.

$L_p$ = plug length, cm.

$M$ = molecular weight, g./g. mole

$N_G$ = gas-phase–flow rate, mg. moles/sec.

$N_S$ = adsorbed-layer flow rate, mg. moles/sec.

$N_T$ = total flow rate, mg. moles/sec.

$p, p'$ = gas-phase pressure, mm. Hg, dynes/sq. cm.

$\Delta p$, $\Delta p'$ = gas-phase pressure drop, mm. Hg, dynes/sq. cm.

$P_G$ = gas-phase permeability, $N_G L_p/\Delta p A_p$, mg. moles/(sec.)(mm. Hg)(cm.)

$P_T$ = total permeability, $N_T L_p/\Delta p A_p$, mg. moles/(sec.)(mm. Hg)(cm.)

$r$ = radius of capillary, cm.

$R$ = gas constant

$s_s$ = specific surface of solid over which adsorbed molecules are mobile, sq. cm./g.

$T$ = temperature, °K.

$u$ = average rate of movement of adsorbed molecules past the solid surface, (moles/sec.)/(moles/cm.), cm./sec.

$u_p$ = component of film "velocity" $u$ in direction of net flux or along plug length, cm./sec.

$x$ = amount adsorbed, mg. moles/g.

### Greek Letters

$\Delta x$ = difference in amounts adsorbed on two faces of plug, mg. moles/g.

$\lambda$ = mean free path at mean gas pressure level in system, cm.

$\mu$ = gas viscosity, poise

$\rho_{app}$ = apparent density of solid, g./cc.

$\phi$ = spreading pressure, dyne/cm.

## LITERATURE CITED

1. Babbitt, J. D., *Can. J. Res.*, **28A**, 449 (1950).
2. Barrer, R. M., *J. Phys. Chem.*, **57**, 35 (1953).
3. ———, and J. A. Barrie, *Proc. Roy. Soc.* (London), **A213**, 250 (1952).
4. Carman, P. C., *ibid.*, **203**, 55 (1950).
5. *Ibid.*, **A211**, 526 (1952).
6. ———, and P. leR. Malherbe, *ibid.*, **A203**, 165 (1950).
7. Carman, P. C., and F. A. Raal, *ibid.*, **A209**, 38 (1951).
8. Clausing, P., *Ann. physik.*, **7**, 489 (1930).
9. Damkohler, G., *Z. Phys. Chem.*, **A174**, 222 (1935).
10. Emmett, P. H., and T. W. DeWitt, *J. Am. Chem. Soc.*, **65**, 1253 (1943).
11. Flood, E. A., R. H. Tomlinson, and A. E. Leger, *Can. J. Chem.*, **30**, 389 (1952).
12. *Ibid.*
13. Fowler, R., and E. A. Guggenheim, "Statistical Thermodynamics," Chap. 10, University Press, Cambridge (1952)
14. Haul, R., *Z. angew. Chem.*, **62**, 10 (1950).
15. Hodgins, J. W., E. A. Flood, and J. R. Dacey, *Can. J. Res.*, **24B**, 167 (1946).
16. Hoogschagen, J., *Ind. Eng. Chem.*, **47**, No. 5, 906 (1955).
17. Huckins, H. E., and Karl Kammermeyer, *Chem. Eng. Progr.*, **49**, 180 (1953).
18. Jeans, J. H., "An Introduction to the Kinetic Theory of Gases," University Press, Cambridge (1946).
19. Knudsen, M., *Ann. physik.*, **28**, 75 (1909).
20. Russell, J. L., Sc.D. thesis, Mass. Inst. Technol., Cambridge (1955).
21. Sears, G. W., *J. Chem. Phys.*, **22**, No. 7, 1253 (1954).
22. Tomlinson, R. H., and E. A. Flood, *Can. J. Res.*, **26B**, 38 (1948).
23. Wicke, E., and R. Kallenback, *Kolloid Z.*, **97**, 135 (1941).
24. Wicke, E., and U. Voight, *Z. angew. Chem.*, **B19**, 94 (1947).
25. Wheeler, A., "Advances in Catalysis," vol. 3, p. 249, Academic Press, New York (1951).

*Manuscript submitted November, 1956; revision received September 6, 1957; paper accepted September 16, 1957.*